Dalton Transactions

PAPER

View Article Online
View Journal | View Issue

Open Access Article. Published on 05 April 2016. Downloaded on 6/13/2026 1:55:29 AM.
This article is licensed under a Creative Commons Attribution 3.0 Unported Licence.

CrossMark click for updates

Cite this: *Dalton Trans.*, 2016, **45**, 8099

Coordination of Zn^{2+} and Cu^{2+} to the membrane disrupting fragment of amylin†

M. Rowińska-Żyrek

Received 16th February 2016,
Accepted 4th April 2016

DOI: 10.1039/c6dt00628k

www.rsc.org/dalton

Amylin, a small peptide co-secreted from pancreatic β-cells together with insulin, is one of the hallmarks of type II diabetes. In the course of this disease, it misfolds into small oligomers or into an aggregated β-sheet amyloid fiber. The misfolding mechanism is not yet well understood, but it is clear that metal ions such as zinc and copper play an important role in the process. In this work, the coordination chemistry of Zn^{2+} and Cu^{2+} with the membrane-disrupting part of amylin ($amylin_{1-19}$) is discussed. Cu^{2+} alters the structure of $amylin_{1-19}$ only locally, by binding to His18 imidazole and to three preceding amides at the N-terminal side of this residue. Zn^{2+} binds to the imidazole of His18 and the amine group of Lys1, imposing a kink in the peptide between these residues. This zinc-induced kink might be a partial explanation of the formation of prefibrillar oligomeric aggregates of amylin, which are much more toxic to β-cells than large fibrillar deposits.

Introduction

Nowadays, the impact of metal ions on the structure and function of biomolecules has become undoubtable. Understanding the relationship between metal coordination abilities of certain proteins can help explain the molecular basis and, in turn, various macroscopic symptoms present in the course of illnesses. Metal coordination abilities of amyloid beta, α-synuclein or the prion protein in Alzheimer's, Parkinson's and prion disease could be good examples. These proteins which are the hallmarks of the diseases are all linked by being related to metal-coordinated amyloidogenic peptides.[1,2] Such peptides undergo a misfolding process from a random coil; their secondary structure is changed into an α-helical intermediate prior to a conformational change into a β-sheet, which then aggregates to form elongated fibers.[3,4] For decades, there has been inconsistency in whether the presence of excess metal ions (such as Cu^{2+}, Zn^{2+} or Fe(III) and Al^{2+}) triggers or hinders the pathological deposition of amyloid deposits in the brain.[5–9]

In the beginning of the initial debate, the prevailing opinion suggested that the excess of metal ions is the trigger for misfolding, and often, chelation therapy was even suggested.[10] The process was later found to be much more complicated, involving not only metal coordination and disruption of metal homeostasis, but also various other factors, such as the interaction of hydrophobic regions or interactions with membranes that are also factors which trigger the formation of the thermodynamically unfavored nucleus, by which fiber formation is triggered.[11]

There are numerous parallels between amyloidogenic proteins involved in neurodegenerative diseases and a small polypeptide involved in glucose regulation – amylin, also known as the islet amyloid polypeptide (IAPP). Amylin is a 37 residue peptide, which is co-secreted from pancreatic β-cells together with its synergistic partner, insulin, and stored in the secretory granules of the islets of Langerhans in pancreatic β-cells.[12,13] Amylin takes part in glucose regulation and appetite suppression, preventing post-prandial spikes in blood glucose levels.[14] It is also an amyloidogenic peptide that undergoes misfolding from a monomeric random coil conformation to an aggregated β-sheet amyloid fiber, found in the islet beta cells of over 95% of the patients with type II diabetes (T2D)[15,16] – a common, chronic, degenerative metabolic disease characterized by elevated blood glucose levels, abnormal insulin secretion and insulin resistance, which affects over 300 million people worldwide.[17] The misfolding and amyloid fibril formation of amylin result in the death of islet beta cells and are thought to be important in the pathogenesis of T2D.[18] The aggregation of small amylin oligomers results in oxidative stress and in the disruption of cell membranes.[19–21] An increasing amount of evidence shows that most toxic species are not mature amyloid fibrils, but small oligomers, which most likely cause membrane disruption (another parallel to the proteins involved in neurodegeneration).[22–24]

The native form of amylin is amidated at the C-terminus and has a disulfide bridge between Cys2 and Cys7. The

Faculty of Chemistry, University of Wroclaw, F. Joliot-Curie 14, 50383 Wroclaw, Poland. E-mail: magdalena.rowinska-zyrek@chem.uni.wroc.pl

†Electronic supplementary information (ESI) available. See DOI: 10.1039/c6dt00628k

Open Access Article. Published on 05 April 2016. Downloaded on 6/13/2026 1:55:29 AM.
This article is licensed under a Creative Commons Attribution 3.0 Unported Licence.

hormone peptide comprises three regions: (i) the membrane disrupting fibrillogenic N-terminus (residues 1–19, the fragment studied in this work), which influences the overall kinetics of fibril formation, (ii) the amyloidogenic region (residues 20–29), and the C-terminal part (residues 30–37), which enhances amyloid formation (Fig. 1).

One of the differences between the human and the rat form of the peptide is the H18R substitution (Fig. 1), which results in the change of cytotoxicity on β-cells: the human form can become highly cytotoxic, while the non-aggregating rat amylin has negligible influence on β-cell survival.[25,26] It might also be worth to point out that the N-terminal (1–19) region of the human amylin is toxic like the full-length peptide, but the respective sequence of the rat amylin is not (Fig. 1).[27,28]

It is clear that amylin is very prone to aggregation.[29] Why doesn't this process occur *in vivo*, in the granules where it is stored in very high millimolar concentrations? There are several compounds in the granule that prevent amylin from fibrilising under these conditions: (i) the relatively low pH of the granule (pH = 6.0), (ii) the high concentration of zinc (~14 mM) and (iii) the high concentration of insulin (~4 times more than amylin).

The increasing number of diabetic patients causes an elevated amount of attention drawn towards understanding the molecular basis of the disease. As a result of this, numerous recent studies prove that the presence of Zn^{2+} and Cu^{2+} can inhibit the aggregation of amylin, although the underlying mechanism is far from being understood.[29,30] Zinc is of particular interest, since its concentration in pancreatic β-cells is one of the highest in the body, and since zinc deficiency is quite a common symptom of type II diabetes.[31] What is already clear is the fact that the presence of zinc inhibits the membrane disruption ability of amylin and reduces the amount of formed amyloids, but it does not alter the morphology of the fibers. It is interesting that zinc has a dual effect on fibrillogenesis of amylin: it increases the lag-time for fibre formation and increases the rate of addition of amylin to existing fibres at high concentrations, while having the opposite effect at lower concentrations.

Some studies show that also copper(II) levels are significantly elevated in diabetic patients,[32,33] which suggests a correlation between copper homeostasis and the molecular basis of type 2 diabetes. A local disruption of copper homeostasis triggers the formation of oxidative species, stimulating the production of H_2O_2 with amylin[34] (another parallel to amyloid beta).[35] Several studies correlated the ability of copper(II) to inhibit amylin fibrillation with toxicity,[36,37] and confirmed the non-fibrillogenic nature of the copper(II)–amylin aggregates.[38]

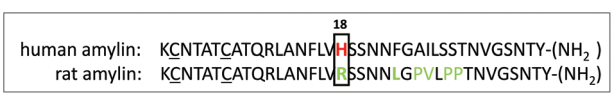

Fig. 1 A comparison of the native sequence of human and rat amylin. Sequential differences are marked in green. Histidine 18 is the potential metal binding site.

This metal has also been found to mediate the membrane-interactions of the 17–29 fragment of amylin.[39]

Recently, the 15–22 fragment was studied by using different spectroscopy techniques, showing that Cu^{2+} anchors to His18 and, which is quite unusual, binds to the subsequent amide groups toward the C-terminus, forming a thermodynamically unfavorable seven-membered chelate ring with an equatorial {3N,O} coordination mode at physiological pH.[40] Copper binding to a monomeric IAPP was expected to compete with conformation changes needed to form β-sheet structures, and thus delay fibril formation.

The interactions of Cu^{2+} with the rat fragments of amylin were also extensively studied, showing the formation of a square planar complex, in which copper(II) is bound to four amide nitrogens.[41]

Knowing the importance of the impact of copper and zinc on the aggregation and membrane disrupting abilities of amylin, this work tries to understand the interactions between Cu^{2+} and Zn^{2+} with the membrane disrupting fragment of human amylin, KCNTATCATQRLANFLVHS-NH_2 (amylin$_{1-19}$), focusing on the thermodynamics of such complex formation and precisely pointing out metal binding sites. The work provides a detailed understanding of the coordination chemistry of amylin–metal interactions and gives insight into bioinorganic chemistry of type 2 diabetes.

Experimental

Synthesis

The C-protected disulphide-bridged amylin$_{1-19}$ (KCNTATCATQRLANFLVHS-NH_2) was purchased from KareBay Biochem (USA) (certified purity: 99.30%) and was used as received. Its purity was checked potentiometrically. $Cu(ClO_4)_2$ and $Zn(ClO_4)_2$ were extra pure products (Sigma-Aldrich); the concentrations of their stock solutions were determined by ICP-MS. The carbonate-free stock solution of 0.1 mol dm^{-3} KOH was purchased from Sigma-Aldrich and then potentiometrically standardized with potassium hydrogen phthalate.

Potentiometric measurements

Stability constants for proton, Cu^{2+} and Zn^{2+} complexes were calculated from titration curves carried out in the pH range 2–11 at 25 °C and ionic strength 0.1 M ($KClO_4$) using a total volume of 3 cm^3. The potentiometric titrations were performed using a Dosimat 665 Metrohm titrator connected to a Metrohm 691 pH-meter and a Metrohm LL Unitrode glass electrode. The thermostabilized glass-cell was equipped with a magnetic stirring system, a microburette delivery tube and an inlet–outlet tube for argon. Solutions were titrated with 0.1 M carbonate-free KOH. The electrodes were daily calibrated for hydrogen ion concentrations by titrating $HClO_4$ with KOH under the same experimental conditions as above. The purities and the exact concentrations of the ligand solutions were determined by the Gran method.[42] The ligand concentration

 This journal is © The Royal Society of Chemistry 2016

Open Access Article. Published on 05 April 2016. Downloaded on 6/13/2026 1:55:29 AM.
This article is licensed under a Creative Commons Attribution 3.0 Unported Licence.

was 1 mM, and the Zn^{2+} and Cu^{2+}-to-ligand ratios were both 1 : 1.

HYPERQUAD 2006 and SUPERQUAD programs were used for stability constant calculations.[43,44] Standard deviations were computed by HYPERQUAD 2006 and refer to random errors only. The constants for hydrolytic Zn^{2+} species were used in these calculations.[45] The speciation and competition diagrams were computed with the HYSS program.[46]

Spectroscopy studies

Solutions were of similar concentrations with respect to those used in the potentiometric studies. Absorption spectra were recorded on a Cary 300 Bio spectrophotometer. Circular dichroism (CD) spectra were recorded on a Jasco J 715 spectropolarimeter in the 800–230 nm range.

The UV-Vis and CD spectroscopy parameters were calculated from the spectra obtained at the pH values corresponding to the maximum concentration of each particular species, on the basis of potentiometric studies.

Mass spectrometry measurements

High-resolution mass spectra were obtained on a BrukerQ-FTMS spectrometer (Bruker Daltonik, Bremen, Germany), equipped with an Apollo II electrospray ionization source with an ion funnel. The mass spectrometer was operated in positive ion mode. The instrumental parameters were as follows: scan range m/z 300–3000, dry gas – nitrogen, temperature 170 °C, and ion energy 5 eV. The capillary voltage was optimized to the highest S/N ratio and it was 4500 V. The small changes in voltage (±500 V) did not significantly affect the optimized spectra. The samples (metal : ligand in a 1 : 1, 1 : 2 and 2 : 1 stoichiometry, $[ligand]_{tot} = 10^{-4}$ M) were prepared in a 1 : 1 acetonitrile–water mixture at pH 5, 7.4 and 9. The variation of the solvent composition down to 5% of acetonitrile did not change the species composition. The sample was infused at a flow rate of 3 μL min^{-1}. The instrument was calibrated externally with a Tunemix™ mixture (Bruker Daltonik, Germany) in quadratic regression mode. Data were processed by using Bruker Compass DataAnalysis 4.0 program. The mass accuracy for the calibration was better than 5 ppm, enabled together with the true isotopic pattern (using SigmaFit) an unambiguous confirmation of the elemental composition of the obtained complex.

NMR measurements

NMR spectra were recorded at 14.1 T on a Bruker Avance III 600 MHz equipped with a Silicon Graphics workstation. The temperatures were controlled with an accuracy of ±0.1 K. Suppression of the residual water signal was achieved by excitation sculpting, using a selective square pulse on water, 2 ms long. All the samples were prepared in a 90% H_2O and 10% D_2O (99.95% from Merck) mixture. Proton resonance assignment was accomplished by 2D ^1H–^1H total correlation spectroscopy (TOCSY) and nuclear Overhauser effect spectroscopy (NOESY) experiments were carried out with standard pulse sequences. Spectral processing and analysis were performed using Bruker TOPSPIN 2.1 and Sparky. The samples of complexes were prepared by adding metal ions to an acidic solution of a ligand (pH 3.5), and the pH was then increased to a higher value.

Results and discussion

Structural and thermodynamic properties of Zn^{2+} and Cu^{2+} complexes with the membrane disrupting part of amylin were studied and compared to each other by using mass spectrometry, potentiometry, and several spectroscopy techniques. Mass spectrometry measurements provided the information on the stoichiometry of the interactions and the combined UV-Vis and CD results allowed us to conclude that the binding mode of copper(II) and the geometry of these species formed in solution and potentiometric titrations were the basis for the determination of precise stability constants and pH-dependent species distribution diagrams for the studied systems. NMR spectra recorded both in the presence and in the absence of metal ions pointed out precise metal binding sites. A combination of all the used methods allowed us to explain coordination geometries and perform thermodynamic analysis.

The K<u>C</u>NTAT<u>C</u>ATQRLANFLVHS-NH_2 peptide ($amylin_{1–19}$) behaves as an LH_3 acid, with the deprotonating groups corresponding to the histidine imidazole, the N-terminal amine group and the lysine side chain group, with pK_a values of 6.04, 7.91 and 10.83, respectively. The cysteine groups are bridged with a disulfide bond, as in the wild type form of amylin, and the C-terminal serine is amidated, in order to be a better mimic of the full-length amylin.

$Amylin_{1–19}$ shows an NMR behavior typical of a disordered peptide. NMR spectra recorded at different pH values and temperatures did not suggest any specific rearrangements of the apo peptide.

Mass spectrometry proves that $amylin_{1–19}$ forms only mononuclear complexes with both copper and zinc ions. ESI-MS peak assignments were based on the comparison between the precise calculated and experimental m/z values and their isotopic patterns. The prevailing signals correspond to the free ligand (m/z = 1038.6, z = 2+) and to the chloride adducts of equimolar complexes with Cu^{2+} (m/z = 1088.5, z = 2+) and with Zn^{2+} (m/z = 1089.1, z = 2+) (Fig. S1†). The signals are most abundant under all the studied pH conditions (pH 5, 7.4 and 9), and also when 1 : 2, 1 : 1 and 2 : 1 metal to ligand ratios are analyzed. Other minor signals correspond to various chloride and sodium adducts of the free ligand and of their metal complexes.

There are major differences in the coordination mode of amylin copper and zinc complexes. The only parallel for both metals is the first anchoring site – the His18 imidazole; the remaining coordinating groups are different for the two metals.

In the case of copper species, the first complex observed at low pH, CuH_2L, involves only His18 in binding – this is clearly visible in the NMR spectra (Fig. 2A), whereafter the addition of 0.3 Cu^{2+} equivalents, only the aromatic imidazole protons are

Open Access Article. Published on 05 April 2016. Downloaded on 6/13/2026 1:55:29 AM.
This article is licensed under a Creative Commons Attribution 3.0 Unported Licence.

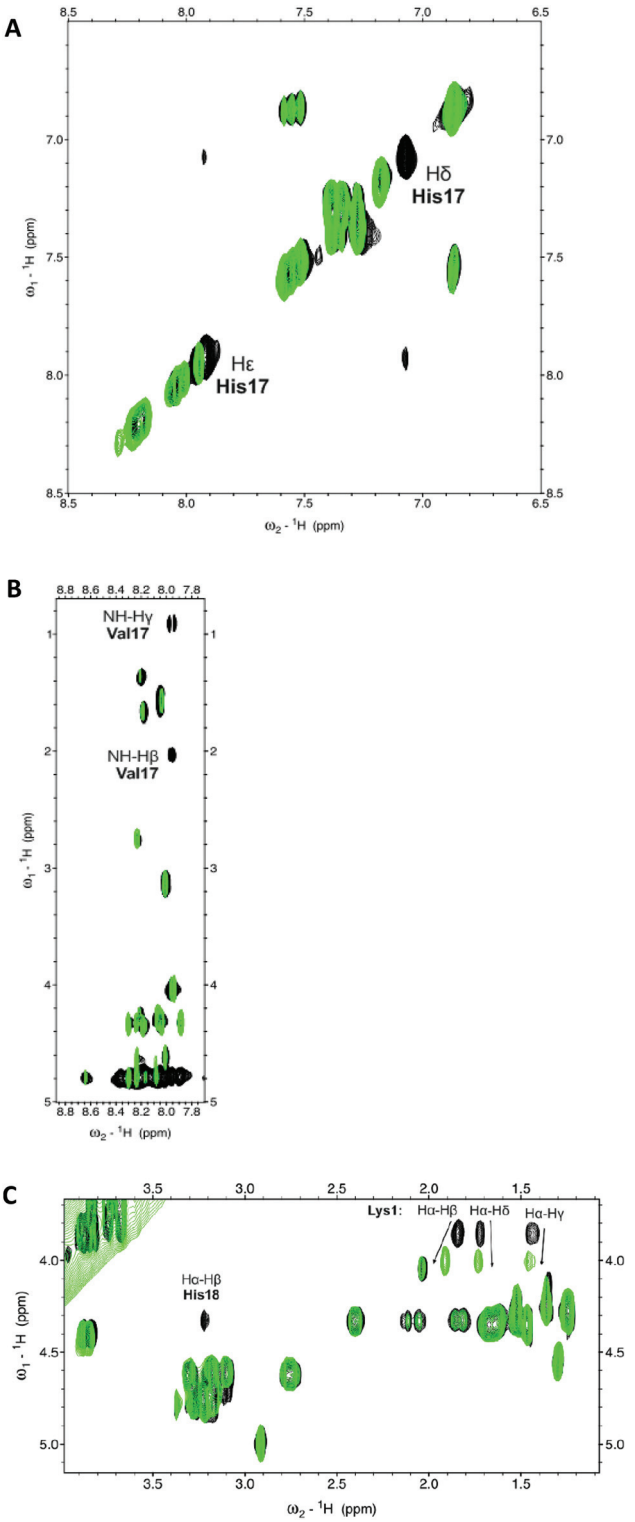

Fig. 2 Selected regions of $^{1}H-^{1}H$ TOCSY spectra of 3 mM amylin$_{1-19}$, T = 298 K, in the absence (black contours) and in the presence (green contours) of metal ions; (A) 0.3 Cu^{2+} equivalents, pH 4; (B) 0.3 Cu^{2+} equivalents, pH 5.5; (C) 1 Zn^{2+} equivalent, pH 7.2.

broadened (since copper is a paramagnetic metal ion, a reasonably small amount of this metal causes selective broadening of the residues involved in binding). The coordination mode is further confirmed by a d–d band at 655 nm in UV-Vis spectroscopy, and by the lack of pronounced circular dichroism signals (Table 1, Fig. S2 and S3†). However, the possible co-existence of minor CuHL species cannot be unequivocally excluded.

Above pH 5, drastic changes can be observed in all spectroscopy methods. The UV-Vis band undergoes a blue shift to 560 nm, and the CD spectra are typical of a $\{N_{im},2N^{-}\}$ coordination (Table 1, Fig. S2 and S3†). Also, selective broadening on NH gamma and NH beta of Val17 observed on the NMR spectra strongly supports the involvement of amide nitrogens in binding (Fig. 2B).

Above pH 6, the CuL complex deprotonates to $CuH_{-1}L$, with a pK_a of 5.39 (Fig. 3A). The strong blue shift and increase in intensity in the CD (from 635 to 595 nm, Table 1 and Fig. S3†) and UV-Vis spectra (from 560 to 545 nm, Table 1 and Fig. S2†) confirm the involvement of a third amide in the coordination, resulting in $\{N_{im}, 3N^{-}\}$ binding mode. This mode does not change with the further increase of pH; pK_a constants of 8.11 and 9.74 correspond to the deprotonation of the N-terminal amine and of the side chain of lysine, respectively; both the groups do not participate in binding (Table 1).

The coordination of Zn^{2+} to amylin$_{1-19}$ differs significantly when compared to that of Cu^{2+}; for ZnH_2L, the anchoring site is the histidine imidazole, just as it was in the first complex observed for copper at low pH. However, in the species observed at a physiological pH (with a maximum at pH 7.2), ZnHL, the imidazole nitrogen and the N-terminal amino group are the residues which are directly involved in coordination; the vacant zinc binding sites are occupied by water molecules. The pK_a value of 6.27 strongly suggests the involvement of this group in binding (the corresponding pK_a for the free ligand = 7.91, Table 1). NMR spectroscopy confirms the $\{N_{im},NH_2\}$ binding mode. The addition of Zn^{2+} to amylin$_{1-19}$ causes selective line broadening of His18 Hα–Hβ correlation and a broadening and shift of the N-terminal Lys1 Hα–Hβ, Hα–Hδ and Hα–Hγ NMR signals (Fig. 2C). The terminal amine protons are not visible in either the metal bound or the apo form of the peptide, most probably due to a fast water exchange.

The ZnHL complex dominates in solutions up to pH 8. At higher pH, two stepwise deprotonations with the corresponding pK_a values of 8.07 and 8.22 occur (Fig. 3B and Table 1). Most likely, those two protons arise from two water molecules, present in the two vacant coordination sites not occupied by peptide residues. This scenario is very likely, since Zn^{2+} is not able to deprotonate amide nitrogens, in contrast to Cu^{2+}. Another scenario could include the carbonyl oxygen of His18 or Lys1 having a stabilization role in the coordination of Zn^{2+}.

The binding mode does not change with the increase of pH; the $ZnH_{-2}L$ complex results from the deprotonation of the unbound lysine residue (with a pK_a value of 9.84).

It becomes obvious that His18 is crucial for the coordination of both copper and zinc to amylin$_{1-19}$. This was expected, since it was already shown in previous studies that

 This journal is © The Royal Society of Chemistry 2016

Open Access Article. Published on 05 April 2016. Downloaded on 6/13/2026 1:55:29 AM.
This article is licensed under a Creative Commons Attribution 3.0 Unported Licence.

Table 1 Potentiometric and spectroscopy data for proton, Cu^{2+} and Zn^{2+} complexes of amylin$_{1-19}$

			UV-Vis		CD	
Species	log β	pK_a	λ/nm	ε/M^{-1} cm^{-1}	λ/nm	$\Delta\varepsilon$/M^{-1} cm^{-1}
HL	10.83	10.83 (Lys)				
H_2L	18.74	7.91 (N-t)				
H_3L	24.78	6.04 (His)				
Cu^{2+} complexes						
CuH_2L	24.92 (2)		655	36	279	−0.09
					317	−0.06
					690	−0.11
CuL	14.19 (2)	5.39 (amide)	560	123	288	−27.3
					319	6.74
					495	2.72
					635	11.56
$CuH_{-1}L$	8.80 (3)	8.11 (N-t)	545	145	292	−18.90
					316	8.22
					503	8.06
					595	−17.75
$CuH_{-2}L$	0.69 (4)	9.74 (Lys)	540	158	295	−9.50
					316	17.58
					495	6.13
					570	−18.49
$CuH_{-3}L$	−9.05 (5)		535	154	292	−11.05
					316	19.45
					560	−19.21
Zn^{2+} complexes						
ZnH_2L	21.33 (2)	6.27 (N-t)				
ZnHL	15.06 (2)	8.07 (H_2O)				
ZnL	6.99 (4)	8.22 (H_2O)				
$ZnH_{-1}L$	−1.23 (4)	9.84 (Lys)				
$ZnH_{-2}L$	−11.07 (7)					

the binding of zinc to amylin causes a local disruption of the secondary structure in the vicinity of His-18.[47] Biological studies showed that the substitution of this residue to arginine severely reduces the membrane disrupting ability of the 1–19 fragment.[48] The situation becomes very similar after the addition of Zn^{2+} to the full length amylin–membrane disruption also becomes far less pronounced. Both the H to R substitution and zinc binding change the overall charge distribution of the peptides – most likely, such peptides would be more surface associated, since the positive His-18 imidazole would make it impossible for them to penetrate into the hydrophobic core of a lipid bilayer. Also, zinc may create an energetic barrier for the formation of amyloids by promoting the formation of prefibrillar aggregates and thus inhibiting the formation of amyloid fibrils.[49,50] It is worth keeping in mind that (just as it was in the case of amyloid β) mature amyloid fibers show relatively little toxicity to β-cells, and most likely the small, prefibrillar aggregates are the toxic species.[23]

It is tempting to suggest that the zinc–amylin binding mode described in this work might be at least a partial explanation of how these prefibrillar aggregates are formed – the coordination mode which involved the imidazole of His18 and the amine group of Lys1 imposes a kink between those residues (Fig. 4). This special structure might be the thermodynamical basis of prefibrillar aggregate formation. Zinc is bound to His18 and Lys1 at a physiological pH (ZnHL species, in our case, with a maximum abundance at pH 7.2). Literature data show that at a similar pH, the presence of low concentrations of Zn^{2+} in the incubation solution decreases the rate of amylin amyloid formation, whereas a higher zinc concentration has an opposite effect.[48]

Again, it can be hypothesised that in excess of zinc, more than one Zn^{2+} ion can be bound to the peptide (*e.g.* one to His18 and another to the N-terminal amine of Lys1) – in this case, the special kink observed in the case of mononuclear species would no longer be present.

Copper, on the other hand, alters the structure of amylin$_{1-19}$ only locally, by binding to His18 imidazole and to three preceding amides at the N-terminal side of this residue (Fig. 4). It is quite a common binding mode for Cu^{2+}, and in the case of amylin$_{1-19}$ ($CuH_{-1}L$), it already starts to prevail in solution at pH 6. This coordination mode is different from the one reported by Rivillas-Acevedo *et al.*;[40] here copper deprotonated amides from the 15–24 amylin fragment are towards the C-terminus of the peptide. Clearly, the membrane disrupting amylin$_{1-19}$ region has only one amide that can be deprotonated by Cu(II), once it is bound to His18 and the data cannot be directly compared to that from Rivillas-Acevedo's work. The binding mode of the highly prone to aggregation full length amylin requires more studies, *e.g.* on the non-aggregating analogue – pramlintide.

Open Access Article. Published on 05 April 2016. Downloaded on 6/13/2026 1:55:29 AM.
This article is licensed under a Creative Commons Attribution 3.0 Unported Licence.

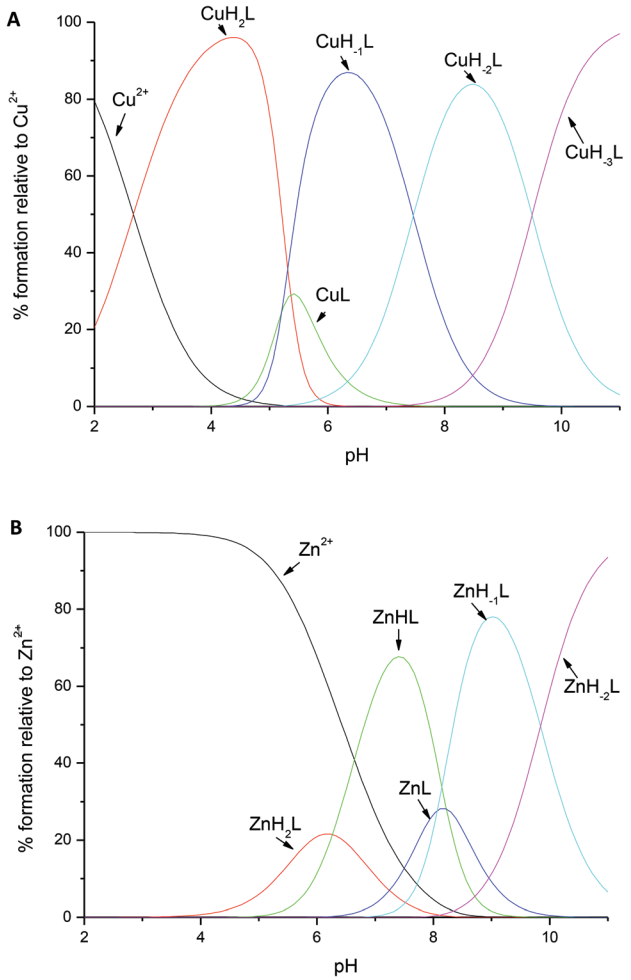

Fig. 3 Distribution diagrams for the formation of (A) Cu^{2+} and (B) Zn^{2+} complexes with amylin$_{1-19}$ at 25 °C and I = 0.1 M. [M^{2+}] = 0.5 × 10^{-3} M; M/L molar ratio = 1 : 1.

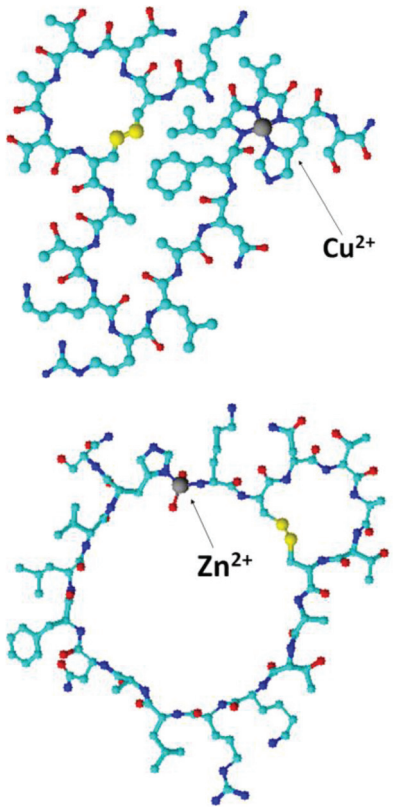

Fig. 4 Suggested binding modes of Cu^{2+} and Zn^{2+} complexes at pH 7.2. Explicit hydrogens are omitted for clarity.

Biological studies emphasize the role of copper-dependent generation of H_2O_2, which was found to directly contribute to the toxicity of human amylin.[51,52] Again, a similar scenario was observed in the case of β-amyloid-copper or prion-copper complexes.[7,53] Does similar coordination chemistry result in a similar biological outcome? Most probably, numerous biological studies and a detailed kinetical description of the amyloid aggregation in the presence of metal ions are necessary, before the answer to this question becomes something more than a very far-reaching hypothesis about the protective role of copper–amylin complex *in vivo*.

Conclusions

Misfolding processes of certain proteins are a common hallmark of numerous diseases. Most common examples are those involved in neurodegeneration – α-synuclein, β-amyloid, huntingtin or the prion protein. For almost two decades, we have been experiencing an ongoing debate about the impact of metal ions on the molecular basis and, in turn, on the course of these illnesses. Recently, a similar discussion has been started for amylin, which shows numerous parallels to metal binding amyloid-forming neuro-proteins.

This work summarizes the details of Zn^{2+} and Cu^{2+} coordination to the membrane-disrupting fragment of amylin and amylin$_{1-19}$. The anchoring site for Cu^{2+} is His18, and at physiological pH, the histidine imidazole and three amides are in the first coordination sphere. Such a typical, square-planar copper complex might contribute to the generation of H_2O_2, which is one of the factors responsible for the toxicity of human amylin. From the point of view of bioinorganic chemistry, the binding mode of Zn^{2+} to amylin$_{1-19}$ seems to be much more interesting – at physiological pH, it is bound to His18 imidazole and to the N-terminal amine group of Lys1. This type of binding induces a kink in the peptide backbone, which might be the first step of prefibrillar aggregate formation.

This work gives us very precise details about the coordination of copper and zinc to the membrane disrupting fragment of amylin, but in the end, it brings up even more questions that still need to be answered: does the binding of zinc and copper indeed have an influence on the pathogenesis of amylin? How does it influence the aggregation of the full-length amylin? And, above all – are the metal-bound aggregates the cause, or rather the consequence of T2D?

This journal is © The Royal Society of Chemistry 2016

Open Access Article. Published on 05 April 2016. Downloaded on 6/13/2026 1:55:29 AM.
This article is licensed under a Creative Commons Attribution 3.0 Unported Licence.

Acknowledgements

The author would like to express her thankfulness to Ms. Agnieszka Przybyła for her skillful assistance in solution studies. The work was supported by the National Science Centre (nr UMO-2014/13/D/ST5/02868) and by the Ministry of Science and Higher Research (1493/M/WCH/15).

References

1 R. A. Floyd and D. A. Butterfield, *Proc. Natl. Acad. Sci. U. S. A.*, 1994, **91**, 3270.
2 B. J. Tabner, S. Turnbull, O. El-Agnaf and D. Allsop, *Curr. Top. Med. Chem.*, 2001, **1**, 507.
3 G. Yamin, C. B. Glaser, V. N. Uversky and A. L. Fink, *J. Biol. Chem.*, 2003, **278**, 27630.
4 C. Talmard, R. L. Yona and P. Faller, *J. Biol. Inorg. Chem.*, 2009, **14**, 449.
5 E. Gaggelli, H. Kozłowski, D. Valensin and G. Valensin, *Chem. Rev.*, 2006, **106**, 1995.
6 H. Kozłowski, M. Łuczkowski, M. Remelli and D. Valensin, *Coord. Chem. Rev.*, 2012, **256**, 2129.
7 M. Rowińska-Żyrek, M. Salerno and H. Kozłowski, *Coord. Chem. Rev.*, 2015, **284**, 298.
8 S. S. Leal, H. M. Botelho and C. M. Gomes, *Coord. Chem. Rev.*, 2012, **256**, 2253.
9 B. R. Roberts, T. M. Ryan, A. I. Bush, C. L. Masters and J. A. Duce, *J. Neurochem.*, 2012, **1**, 149.
10 A. Gaeta and R. C. Hider, *Br. J. Pharmacol.*, 2005, **146**, 1041.
11 M. Jucker and L. C. Walker, *Ann. Neurol.*, 2001, **70**, 532.
12 S. E. Khan, D. A. D'Alessio, M. W. Schwartz, W. Y. Fujimoto, J. W. Ensinck, G. J. J. Taborsky and D. J. J. Porte, *Diabetes*, 1990, **5**, 634.
13 A. Kanatsuka, H. Makino, H. Ohsawa, Y. Tokuyama, T. Yamaguchi, S. Yoshida and M. Adachi, *Fed. Eur. Biochem. Soc. J.*, 1989, **259**, 199.
14 T. K. Reda, A. Geliebter and F. X. Pi-Sunyer, *Obes. Res.*, 2002, **10**, 1087.
15 P. Westermark and E. Wilander, *Diabetologia*, 1978, **15**, 417.
16 J. W. Hoppener and C. J. Lips, *Int. J. Biochem. Cell Biol.*, 2006, **38**, 726.
17 J. M. Olefsky, in *Endocrinology*, ed. L. J. De Groot, Saunders, London, 1989, vol. 2, p. 1369.
18 J. W. Hoppener, B. Ahren and C. J. Lips, *N. Engl. J. Med.*, 2000, **343**, 411.
19 K. Ono, M. M. Condron and D. B. Teplow, *Proc. Natl. Acad. Sci. U. S. A.*, 2009, **106**, 14745.
20 J. R. Brender, S. Salamekh and A. Ramamoorthy, *Acc. Chem. Res.*, 2012, **45**, 454.
21 S. A. Jayasinghe and R. Langen, *Biochemistry*, 2005, **44**, 12113.
22 J. R. Brender, E. L. Lee, K. Hartman, P. T. Wong, A. Ramamoorthy, D. G. Steel and A. Gafni, *Biophys. J.*, 2011, **100**, 685.
23 C. Haass and D. J. Selkoe, *Nat. Rev. Mol. Cell Biol.*, 2007, **8**, 101.
24 J. P. Cleary, D. M. Walsh, J. J. Hofmeister, G. M. Shankar, M. A. Kuskowski, D. J. Selkoe and K. H. Ashe, *Nat. Neurosci.*, 2005, **8**, 79.
25 G. Pappalardo, D. Milardi, A. Magri, F. Attanasio, G. Impellizzeri, C. La Rosa, D. Grasso and E. Rizzarelli, *Chem. – Eur. J.*, 2007, **13**, 10204.
26 R. P. R. Nanga, J. R. Brender, J. Xu, G. Veglia and A. Ramamoorthy, *Biochemistry*, 2008, **47**, 12689.
27 A. N. Roberts, B. Leighton, J. A. Todd, D. Cockburn, P. N. Schofield, R. Suttonet, *et al.*, *Proc. Natl. Acad. Sci. U. S. A.*, 1989, **86**, 9662.
28 J. R. Brender, K. Hartman, K. R. Reid, R. T. Kennedy and A. Ramamoorthy, *Biochemistry*, 2008, **47**, 12680.
29 V. Wineman-Fisher, Y. Atsmon-Raz and Y. Miller, *Biomacromolecules*, 2015, **16**, 156.
30 F. Belliaa and G. Grasso, *J. Mass Spectrom.*, 2014, **49**, 274.
31 C. G. Taylor, *BioMetals*, 2005, **18**, 305.
32 A. H. Zargar, N. A. Shah, S. R. Masoodi, B. A. Laway, F. A. Dar, A. R. Khan, F. A. Sofi and A. I. Wani, *Postgrad. Med. J.*, 1998, **74**, 665.
33 T. Naka, H. Kaneto, N. Katakami, T. Matsuoka, A. Harada, Y. Yamasaki, M. Matsuhisa and I. Shimomura, *Endocr. J.*, 2013, **60**, 393.
34 A. Masad, L. Hayes, B. J. Tabner, S. Turnbull, L. J. Cooper, N. J. Fullwood, M. J. German, F. Kametani, O. M. El-Agnaf and D. Allsop, *FEBS Lett.*, 2007, **581**, 3489.
35 D. Schubert, C. Behl, R. Lesley, A. Brack, R. Dargusch, Y. Sagara and H. Kimura, *Proc. Natl. Acad. Sci. U. S. A.*, 1995, **92**, 1989.
36 B. Ward, K. Walker and C. Exley, *J. Inorg. Biochem.*, 2008, **102**, 371.
37 C. E. E. House, T. Patel, L. Wu and P. E. Fraser, *J. Inorg. Biochem.*, 2010, **104**, 1125.
38 A. Sinopoli, A. Magrı, D. Milardi, M. Pappalardo, P. Pucci, A. Flagiello, J. J. Titman, V. G. Nicoletti, G. Caruso, G. Pappalardo and G. Grasso, *Metallomics*, 2014, **6**, 1841.
39 G. Pappalardo, D. Milardi, A. Magri, F. Attanasio, G. Impellizzeri, C. La Rosa, D. Grasso and E. Rizzarelli, *Chem. – Eur. J.*, 2007, **13**, 10204.
40 L. Rivillas-Acevedo, C. Sánchez-López, C. Amero and L. Quintanar, *Inorg. Chem.*, 2015, **54**, 3788.
41 A. David, C. Kallay, D. Sanna, N. Lihi, I. Sovago and K. Varnagy, *Dalton Trans.*, 2015, **44**, 1709.
42 G. Gran, *Acta Chem. Scand.*, 1950, **4**, 559.
43 P. Gans, A. Sabatini and A. Vacca, *J. Chem. Soc., Dalton Trans.*, 1985, 1195.
44 P. Gans, A. Sabatini and A. Vacca, *Talanta*, 1996, **43**, 1739.
45 L. Pettit and H. K. J. Powell, *The IUPAC Stability Constants Database*, IUPAC, London, 1992–2002.
46 L. Alderighi, P. Gans, A. Ienco, D. Peters, A. Sabatini and A. Vacca, *Coord. Chem. Rev.*, 1999, **184**, 311.
47 J. R. Brender, K. Hartman, R. P. R. Nanga, *et al.*, *J. Am. Chem. Soc.*, 2010, **132**, 8973.

48 J. R. Brender, K. Hartman, K. R. Reid, R. T. Kennedy and A. Ramamoorthy, *Biochemistry*, 2008, **47**, 12680.
49 J. R. Brender, J. Krishnamoorthy, G. M. L. Messina, *et al.*, *Chem. Commun.*, 2013, **49**, 3339.
50 S. Salamekh, J. R. Brender, S. J. Hyung, *et al.*, *J. Mol. Biol.*, 2011, **410**, 294.
51 A. Masad, L. Hayes, B. J. Tabner, *et al.*, *FEBS Lett.*, 2007, **581**, 3489.
52 A. Masad, B. J. Tabner, J. Mayes and D. Allsop, *Free Radicals Biol. Med.*, 2011, **51**, 869.
53 B. J. Tabner, O. M. A. El-Agnaf, S. Turnbull, *et al.*, *J. Biol. Chem.*, 2005, **280**, 35789.

Open Access Article. Published on 05 April 2016. Downloaded on 6/13/2026 1:55:29 AM.
This article is licensed under a Creative Commons Attribution 3.0 Unported Licence.

This journal is © The Royal Society of Chemistry 2016